

Adaptive collective decision-making in limited robot swarms without communication

Serge Kernbach¹, Dagmar Häbe², Olga Kernbach¹, Ronald Thenius³,
Gerald Radspieler³, Toshifumi Kimura⁴ and Thomas Schmickl³

Abstract

In this work we investigate spatial collective decision-making in a swarm of microrobots, inspired by the thermotactic aggregation behavior of honeybees. The sensing and navigation capabilities of these robots are intentionally limited; no digital sensor data processing and no direct communication are allowed. In this way, we can approximate the features of smaller mesoscopic-scale systems and demonstrate that even such a limited swarm is nonetheless able to exhibit simple forms of intelligent and adaptive collective behavior.

Keywords

adaptive behaviour, collective decision making, collective intelligence, robot swarm

1. Introduction

Collective autonomous systems fascinate by their capability for well-organized group behavior, large-scale coordination, collective decision-making and collective efficiency (Kernbach, 2012). These capabilities suggest a collective macroscopic intelligence created by interactions among the elements of collective systems. As demonstrated by many natural physical and biological systems, this collective intelligence can appear even when the elements are very limited in terms of sensing, communication and computation (Bonabeau et al., 1999). Miniaturization of robotic technology, in particular, the transition from mini (10^{-2} – 10^{-3} m) to mesoscopic (10^{-3} – 10^{-4} m) scale raises questions about achieving intelligent behavior in such tiny systems.

In this work we argue that a simple form of collective intelligence can be achieved when all elements are able (a) to take a common decision, for example to move to spatial locations with a larger amount of resources; and (b) to adapt their collective behavior to a dynamic environment, for example when resources are changing. For example, such behavior is typical of bacterial microrobots (Martel et al., 2009). Considering non-mechatronic embodiments at the mesoscopic scale, such as protocells (Fellermann et al., 2007), polypeptide vesicles (Bellomo et al., 2004) or functionalized particles (Caruso, 2001), we see that such elements have no peer-to-peer communication (we assume chemotaxis), no long-range sensors, no digital microcontroller, no digital memory and a very simple, even passive,

locomotive system, resulting in the random motion of such elements. These elements can physically interact with each other by means of collisions, can be attracted to or repelled by each other, can perceive some sensory quality (usually light or temperature (Liu et al., 2005)) and have a simple sensor–actor coupling, allowing mapping between the sensing and locomotive parameters.

At first glance, social organisms, even in their most primitive form (e.g. bacteria (Camazine et al., 2001) or slime mold (Nakagaki, 2001)), have little in common with the mesoscopic world, and even less so higher organisms which usually have a sophisticated sensory system and employ direct and indirect communication on various channels. However, their information about the state of the meta-organism (be it a swarm, a colony, a flock or any other manifestation) is usually very limited and collective dynamics do not arise from directed actions but from individual adaptive responses to environmental changes (Bonabeau et al.,

¹Institute of Parallel and Distributed Systems, University of Stuttgart, Stuttgart, Germany

²Fraunhofer Institute for Industrial Engineering IAO, Stuttgart, Germany

³Department for Zoology, University of Graz, Graz, Austria

⁴School of Human Science and Environment, University of Hyogo, Himeji, Hyogo, Japan

Corresponding author:

Serge Kernbach, Institute of Parallel and Distributed Systems, University of Stuttgart, Universitätsstr. 38, D-70569 Stuttgart, Germany. Email: Serge.Kernbach@ipvs.uni-stuttgart.de

1997). There is often a feedback loop between environmental and collective dynamics and a dynamical process that changes the state of an entire swarm may be started by one or a few individuals manipulating the environment on a minimal scale (e.g. stigmergy (Bonabeau et al., 1999; Dorigo et al., 2000)). This is especially true for social insects, whose collective capabilities are elevated above individual capabilities more than in any other social organism. While a number of insect species are occasionally associated in groups and exhibit forms of collective behavior (e.g. cockroaches (Ame et al., 2004; Jeanson et al., 2004; Leoncini and Rivault, 2005), bark beetle (Deneubourg et al., 1990b) or fire bugs), the group of hymenopterans (e.g. ants, honeybees, bumblebees, wasps) has, alongside termites, brought about the best and most tightly organized collective systems. While ant societies have been more profusely investigated in terms of social behavior (e.g. Wilson, 1980; Deneubourg et al., 1990a; Bonabeau et al., 1998; Lioni et al., 2001; Deneubourg et al., 2002; Martin et al., 2002; Depickere et al., 2004)), honeybees are an especially interesting inspiration for swarm robotics due to their temperature-induced aggregation behavior (Heran, 1952; Sumpter and Broomhead, 2000) which can be easily adopted and reproduced by robots (Schmickl et al., 2008; Schmickl and Hamann, 2010). This behavior can be explained with a simple model that implements limited agents without memory or long-range sensors with merely the capability to measure the local temperature and to discern between a wall and another agent upon collision (Radspieler et al., 2009).

To explore simple forms of collective intelligence in limited mesoscopic systems, we employed a swarm of microrobots. Different physical laws acting at the micro- and meso-levels do not allow the creation of a substantial analogy between behaviors on these levels. However, the re-programmability of microrobots represents an advantage for understanding the principles of using physical constraints in the design of interactions. These microrobots use only one sensor to deliver the value a and the on-board microcontroller calculates a function $f(a)$. This can be done without a microcontroller with an analog circuit or even chemically. The random motion of the microrobots is influenced by $f(a)$ and there is no communication among them. Thus, the capabilities of the platform used are dramatically limited so as to satisfy the “minimality requirements” mentioned.

The collective intelligence of such limited systems is often expressed in the form of spatial activities, for example flocking, aggregation or energy foraging, and is influenced by the environment. These phenomena are frequently observed in biological systems such as honeybee colonies (Camazine et al., 1990). To investigate the spatial properties of collective decision-making we created several scenarios using two light spots to represent energy sources, and dynamically changing their geometry, size and intensity.

A collective system will best ensure its survival by recognizing the energy level of both sources and congregating first in the most “energy-rich” place (examples from insect societies are described by Seeley et al. (1991) and Camazine and Sneyd (1991) for honeybees and Pasteels et al. (1987) for ants). When there are more robots at a spot than can be satisfied with the available energy, the swarm of robots should split up into sections proportioned so as to maximize the total energy income (honeybee colonies solve this task in the way described by Seeley (1989)). Finally, when the intensity or the number of light spots is changed, the swarm has to adapt its behavior and to make new collective decisions. Thus, the robots create a sui generis collective energy homeostasis (Kernbach and Kernbach, 2011). Robots in groups with subcritical swarm density are not able to exhibit these activities, that is, they are typically collective phenomena. The individual behavior of a microrobot is based on an approach (Kernbach et al., 2009) derived from the thermotactic aggregation behavior of honeybees (Crailsheim et al., 1999). Several modifications of this approach are already published by Häbe (2007) and Bodi et al. (2009, 2010); here, we introduce adaptive aggregation and investigate the influence of spatial conditions on collective behavior.

This paper is organized as follows: in Section 2 we introduce a few theoretical considerations regarding collective intelligence and spatial computations. Sections 3 and 4 explain the experimental setup used and the adaptive aggregation strategy. Sections 5 and 6 describe the experiments performed, Section 7 discusses the results obtained and concludes this work.

2. Spatial interactions for adaptive collective behavior

Collective intelligence is often associated with the macroscopic capabilities of coordination among robots, collective decision-making, division of labor, and task allocation within groups (Weiss, 1999) and is primarily defined by interactions among swarm agents. There are two different cases of such interactions. In the first, the agents communicate through a communication channel capable of exchanging semantic messages. From the information exchange, the agents build different types of common knowledge (Halpern and Mosesi, 1990), which underlie the collective intelligence (Kornienko et al., 2005a). In the second case, the macroscopic capabilities are defined by spatial or dynamical conditions in the environment. The system and environment build a closed macroscopic feedback loop, which works in a collective way as a distributed control mechanism. In this case, there is no need for direct communication; the agents interact kinetically or through stigmergy effects (Bonabeau et al., 1999). Despite the differences in emergent capabilities, flexibility, reactivity and other characteristics, both cases are related to collective

intelligence. Considering the limited swarm agents mentioned above, we refer to this second kind of collective intelligence as the environment-based case

To explain the idea of the impact of spatial environment on collective behavior, we involve the notion of mean free path well-known from the kinetic theory of ideal gases. This notion is related to the average distance the moving particle travels between collisions with other particles. In the case of swarm robots, the collisions mean not only physical but also sensing and communication contacts, i.e. robots can perceive and communicate with each other. Since information between swarm robots is primarily transferred at such collisions, the mean free path is useful for estimating the propagation of information, covering areas, consumed energy and other kinetic relations, see e.g. Kernbach and Kernbach (2011), Kernbach et al. (2009, 2012) and Kernbach (2011). This approach does not involve any specific implementation-dependent parameters, thus can be generalized for different swarm systems.

Robots randomly move around the arena and encounter each other. We consider the case of weakly correlated random walk, known e.g. from Renshaw and Henderson (1981) and Byers (2001), where a rotation angle represents a random function of proximity sensing, however the previous direction of motion influences the availability of these sensor data. The used collision-avoidance model is similar to the hard-sphere collision model of particles. We note the time t_r needed for one robot to encounter another robot. The time t_r depends on the geometry of the arena, and several other factors. After two robots encounter each other, they stop and wait t_w before moving on. In this way, they create a cluster. Other robots can be aggregated by the same mechanism, defined by t_r and t_w times. Obviously, the growing and disappearing of the cluster, that is, the aggregation behavior, depends on the relationship between t_r and t_w and in turn on the spatial environmental conditions.

To proceed more formally, let N robots randomly move in the arena of area S , with velocity v . Each robot can detect another robot within its sensing radius R_s . In the extreme case $R_s = 0$, the robots collide physically, somewhat like particles. First, we estimate the maximum time required for one robot to encounter another robot that does not move. The robot, when moving for t seconds, covers an area S_c

$$S_c = 2R_s vt - S_o, \quad (1)$$

where S_o is the area within which the robot overlaps its trajectories. The overlapping area S_o depends on the swarm density D_{sw} , the collision-avoidance behavior of the robot and the geometry of the robot arena. In Kernbach et al. (2012) we represented a general way of calculating the overlapping trajectories using differential images, in particular, obtaining the value S_o for the variable swarm density

$$S_o = \frac{\pi R_s^2 (Nvt)^2 - 4R_s^2 S}{2R_s Nvt} + \frac{2\sqrt{2}vtR_s^3 N}{0.268S}. \quad (2)$$

Since in this work we primarily focus on estimating the worst case for the time required to reach some point on the arena, given by the longest trajectory of a single non-interacting robot, i.e. multiple robots with overlapping of trajectories will reduce t_r , we ignore the area S_o .

In the worst case, two robots will meet when a moving robot covers the whole area $S - N_c \pi R_s^2$, where $N_c \pi R_s^2$ is the area covered by one standing robot $N_c = 1$, that is, the time t_r needed to meet another robot is

$$t_r = \frac{S - N_c \pi R_s^2}{2R_s v}. \quad (3)$$

Obviously,

$$S > N_c \pi R_s^2. \quad (4)$$

Equation (4) restricts the maximum number of robots in the arena. When two robots move, the time until they meet can be calculated in two ways: first, by using the expression (3); or, second, through the number of sensing contacts (Kernbach et al., 2009). The number of sensing contacts in time t in the robotic arena n_s is equal to the average number of robots N in the area S

$$n_s = \frac{2\sqrt{2}R_s vtN}{S}, \quad (5)$$

where v is the speed of motion, $\sqrt{2}$ is the Maxwell coefficient (the collision-avoidance model of robot behavior is similar to the hard-sphere collision model used in the estimation of the mean free path of the particles). Comparing the time from (3) and (5) at $n_s = 1$, we obtain

$$\frac{S - N_c \pi R_s^2}{2R_s v} > \frac{S}{2\sqrt{2}R_s vN}, \quad (6)$$

i.e. the expression (3) approximates the t_r for the worst case for two robots.

As already mentioned, after the robots encounter each other, they wait t_w before moving on. The waiting mechanism can be technologically implemented in many different ways: chemical docking–releasing systems, electrostatic attraction–repelling forces, or simply by stopping the motion of the microrobots for t_w seconds. The waiting robots form a cluster (Kernbach et al., 2009) and these clusters of stopped robots will grow when the waiting time t_w is larger than the time t_r required to achieve the cluster

$$t_w > t_r. \quad (7)$$

The condition (7) has a fundamental role for a further reason: the t_r depends not only on the parameters of the robot, defined by (3), but also on the geometry of the robot arena. Clusters with a smaller reaching time t_r (that is, with a larger probability of encounter), will grow more quickly than those with a larger t_r . In this way, the structures in the spatial distribution of the probability of encounter affect the clustering behavior of the microrobots. The second factor that influences the aggregation behavior, i.e. t_r , is the size,

position and geometry of a cluster. The robots in the middle of a cluster can leave only after the robots on the boundary disaggregate. For the same reason, round clusters exist for longer than elongated clusters of the same number of robots.

2.1. Appearance of spatial structures in the probability of meeting

In this section we demonstrate that the probability of encounter, which defines t_r and thus the condition (7), is not uniformly distributed in the arena. Since it depends on the geometry of the arena and collision avoidance behavior, we performed three series of experiments with simulated agents, honeybees and real robots, see Figure 1(a)–(c). All three collective systems possess different locomotive properties and it is expected that the results will also apply to other cases of spatial collective behavior. In the experiments with software agents we counted the number of collision contacts. For honeybees and robots we determined their distribution in the arena by counting the frequency of detections in the wall zone and in the remaining arena. For comparison we also estimated the frequency of detection in these zones for software agents. The reason for this procedure is to demonstrate the impact of individual behavior (collision avoidance in the case of robots, more complex behaviors in the case of honeybees) on the probability of meeting.

Experiments in simulation were performed with 2 (Figure 1(d)) and 20 (Figure 1(g)) agents. Each has the 8x neighbors model for movement on a 50×50 grid; when meeting any obstacle, they randomly select another direction of movement. As a random function we used the discrete uniform distribution bounded on the region $[0, 7]$ with a constant probability at every value. Such distribution is also called the discrete rectangular distribution (Johnson et al., 2005). It arises when an event can have a finite and equally probable number of outcomes.

The experiments with honeybees were conducted in the form of 121 experiments with approximately one day old honeybees (*Apis mellifera* ssp.), moving singly in a rectangular arena (56.5×38.5 cm) for 15 min each, see Figure 1(b). The ambient temperature was between 32.3°C and 34.6°C and the environment was lit only by infrared (IR) light (> 610 nm), rendering it effectively dark for the bees. We evaluated video recordings of the bees using a visual tracking program for single individuals to determine their location with a temporal resolution of 1/s. We excluded data points from further evaluation if a bee had remained motionless (i.e. a speed < 0.2 cm/s) for more than 5 s. In addition we discarded experiments in which the bee's average speed was less than 1 cm/s or in which the bee was moving for less than 50% of the time, as these are indications for atypical behavior.

For the robot experiments we used real Jasmine robots in a 115×140 cm² arena, see Figure 1(c). We evaluated

Table 1. Proportions of wall zone and arena center and detections of individuals in the respective zones. Honeybees and groups of 20 robots are detected in the wall zone more frequently than would be expected based on the proportions of the zones. Robots in smaller groups are evenly distributed across the arena in accordance with the proportions of the zones.

	Portion of the arena		Relative frequency of detections	
	Wall zone	Center	Wall Zone	Center
1 bee	0.17	0.83	0.34	0.66
2 agents	0.19	0.81	0.2	0.8
2 robots	0.19	0.81	0.21	0.79
20 agents	0.19	0.81	0.36	0.64
20 robots	0.19	0.81	0.37	0.63

recordings of 2 (Figure 1(f)) and 20 (Figure 1(i)) robots using an improved version of the tracking algorithm for multiple individuals described in (Kimura et al., 2011). The temporal resolution of the evaluation was 25 frames/s.

The results of these experiments are summarized in Table 1. The frequency of individuals in each particular zone directly correlates to the potential frequency of collisions between individuals in the respective zone (compare Equations (3) and (5)). We confirmed this correlation in experiments with software agents by observing and counting the number of collision contacts in different areas. Single honeybees, and large groups of simulated agents and real robots, had an evident preference for the wall zone of the arena, which we delineated as a zone of width twice the size of the observed individuals (2 cm in the honeybee arena and 4 cm in the robot arena). In these experiments, the frequency of detections in the wall zone was higher than expected for evenly distributed individuals, see Table 1 and Figure 1(g)–(i) while there was no evident preference for any other part of the arena. We found no difference in the preference for the wall zone when comparing the results of the experiments with single honeybees and groups of 20 agents and robots. Small groups of simulated agents and robots ($n = 2$) did not exhibit a preference for the wall zone, see Figure 1(d) and (f).

There is a close match between the distributions of individual honeybees and larger groups of robots in the arena. However, the behavioral mechanisms leading to these distributions are different, as demonstrated by the distributions of two robots or simulated agents, which indicate that there is no intrinsic preference for the wall zone in their individual locomotion behavior (Figure 1(d) and (f)). The pronounced preference for the wall zone in larger groups of robots (Figure 1(g) and (i)) can be attributed to the robots' collision avoidance, which drives them away from the center of the arena if the robot density is sufficiently high, but away from the wall if robot density is low. The distribution of single honeybees in the arena exhibits a strong bias towards the wall zone (Figure 1(h)). It is unclear whether this bias is

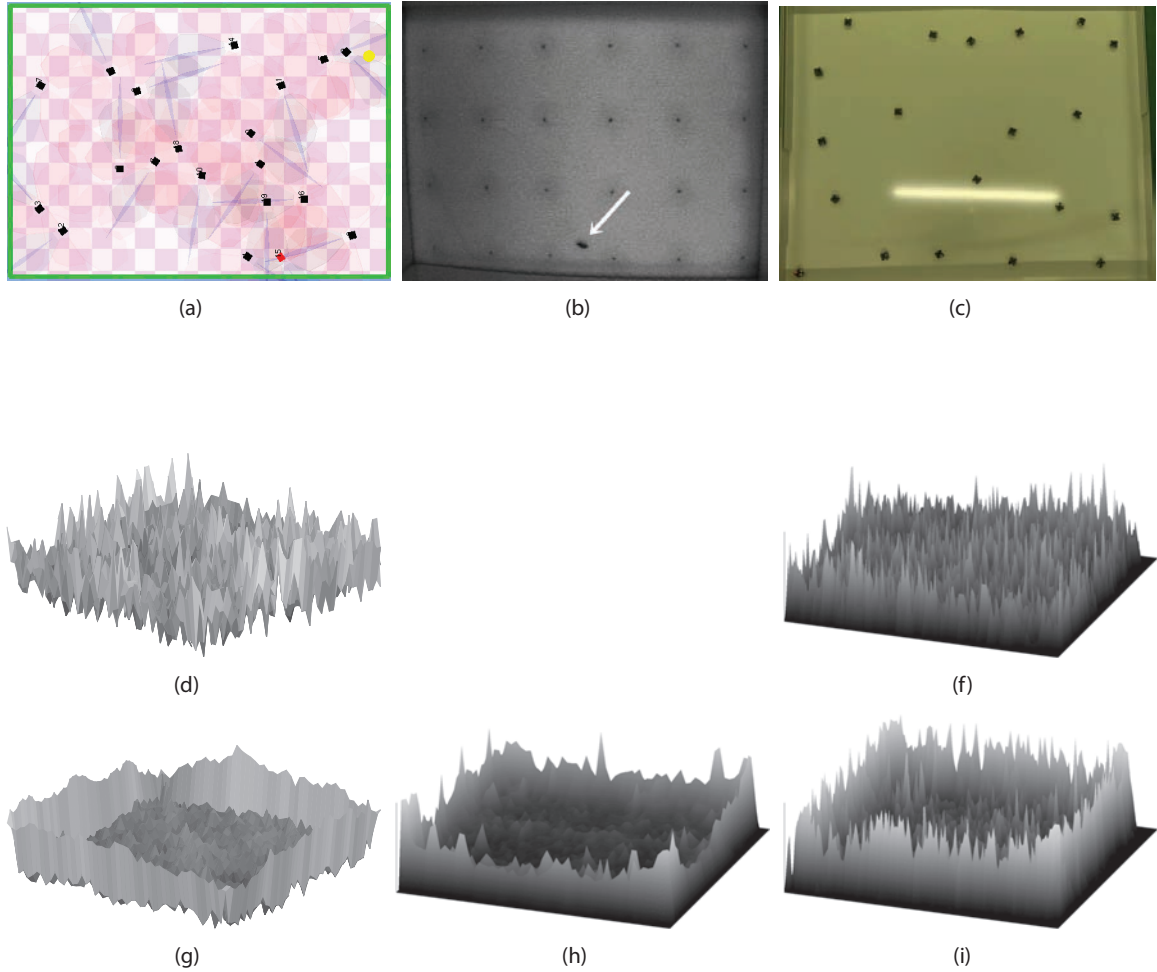


Fig. 1. The appearance of spatial structures in the occurrence of meetings or detections of individuals in the arena: (a) experiments with simulated agents; (b) experiments with a honeybee (arrow); (c) experiments with Jasmine robots. The distribution of the respective individuals in number of detections for: (d) 2 simulated agents; (f) 2 Jasmine robots; (g) 20 simulated agents; (h) 1 honeybee; (i) 10 and 20 Jasmine robots. Values for (f), (h) and (i) are normalized for a detection rate of 1/s. Grid resolution is 1 cm². The sizes of the arenas scale with the body sizes of the tested individuals. There were 88,189 detections of honeybees (h), 28,671 (f) and 309,460 (i) detections of robots were pooled to assemble the distributions. Runaway values caused by individuals remaining excessively long at a specific spot ($n = 5$ in (h), 146 in (i)) were replaced by the average of their neighbors. While honeybees and groups of 20 robots appear disproportionately frequently in the wall zone, no such effect is evident for single robots or pairs of robots (cf. Table 1). Parts (f), (h) and (i) represent the distribution of the number of detections of individual bees and robots in the arena, which is a measure for the probability of encounters between individuals and thus for the probability of cluster formation (see the text).

based on an intrinsic preference for the wall zone in their individual behavioral program or merely on a side-effect of the bees' behavioral response to a collision with the wall. Regardless of the type of agents and the fundamental mechanisms that evoke it, the ultimate bias towards the wall zone explains the increased probability of collisions in this zone. According to Equation (3), the time required to encounter a partner to cluster with is negatively correlated to the number of potential aggregation partners in a given area. Similarly, the number of sensing contacts and thus the probability for the formation of a cluster is positively correlated to the number of individuals in a given

area (Equation (5)). The impact of this parameter increases as the sensor range decreases. For honeybees, whose clustering behavior is based on physical interactions and thus characterized by a short sensor range (two lengths of an antenna), the distribution of individuals gives a reliable prediction for the distribution of clusters in the arena. A similar relationship between distribution of individuals and probability of encounters applies to simulated agents and robots, and since their distribution in larger groups is comparable with that of individual honeybees, their ultimate clustering behavior is comparable as well. Obviously, the fundamental individual behavior that generates the spatial distribution of

individuals underlies algorithms such as division of labor, spatial decision-making, foraging or planning (Kornienko et al., 2003).

2.2. Control of the aggregation behavior

As demonstrated in the previous section, t_r is influenced by spatial structures in the environment. Taking into account the condition (7), changing t_w opens a way to control the aggregation behavior, for example for specific collective decision-making or certain adaptive strategies. First, t_w is correlated with a value a , sensed by a robot, $t_w = f(a)$. In experiments we connected t_w with light intensity and the presence of a seed which initiates aggregation. This seed can either be a specific robot/artefact, see Section 4, or any robot in the arena. The function $f(a)$ was selected as piecewise linear and sigmoid functions, see Figure 2. The values of the variable a vary between 0 (i.e. no seed) up to some maximal values (very close to a seed). Absolute maximum of a is defined by the range of analog-to-digital converter (ADC) set to 255. Second, the function $t_w = f(a)$ can include the second parameter b , which changes the value of t_w depending on a secondary factor. In our experiments we used two different strategies for the secondary factor: first, b depends on the number of robot–robot collisions and second, it adapts step by step the function $t_w = f(a)$ to the average value of the light intensity, see more in Section 4.

When implementing this approach in a swarm of micro-robots, we anticipated several interesting behaviors. First, by changing spatial conditions, we can modify the probability of meetings in the arena and use symmetry-breaking effects in collective decision-making, see Section 4. Second, the robots will be able to distinguish between small and large light spots as well as between spots with different intensity, see Section 5. When the intensity of a light spot was changed dynamically, we expected that robots would migrate to the more intense spot, not from more intense to less intense, see Section 6. In this way, a swarm performs a greedy optimization of the total energy income. Finally, this behavior is sensitive to the swarm density, as indicated by (3). Higher swarm density will result in competition for energy-rich places and division of labor.

These effects will appear when the swarm density satisfies two boundary conditions, defined by subcritical and supercritical swarm densities. As frequently mentioned in the state of the art (e.g. Kernbach, 2012), collective phenomena appear when the swarm density lies inside both boundaries. The lower boundary (subcritical swarm density) appears when the waiting time is less than the time needed to encounter this cluster

$$t_w < t_r. \quad (8)$$

In this case, clusters cannot appear because robots do not have enough time to reach them. To exemplify this value, we consider the case shown in Figure 16(a). Here the cluster can be created only under the lamp, the area of the light spot

is about 1/10 of S . It can be argued that from 10 random attempts, only one time will the robots encounter each other under the lamp. This introduces the factor 10 into the right-hand side of (5). For the estimation we use the maximal value of t_w of 1 minute as demonstrated by Kernbach et al. (2009), $S = 1,400 \times 1,150 \text{ mm}^2$, $R_s = 70 \text{ mm}$ and $v = 300 \text{ mm/s}$. Substituting into (5) and taking into account the factor 10, N is equal to 4.51. Thus, the subcritical swarm density is about five robots for the considered conditions.

The upper boundary (supercritical swarm density) is defined by (6). However, in the case of two lights it appears that areas covered by both light spots $S_{\text{light}_{1,2}}$ is equal to the area covered by N robots

$$S_{\text{light}_{1,2}} = \pi R_s^2 N. \quad (9)$$

For two light spots $S_{\text{light}_{1,2}} = 2S/10$ and $R_s = 70 \text{ mm}$, the supercritical density is achieved at $N = 20.9$ robots. In the case $N > 21$ the area is saturated by robots and their decision behavior is no longer distinguishable. In Section 5.1 we calculated the supercritical density for another placement of lamps and received the supercritical swarm density at $N = 20$. To confirm these estimations, in Section 6 we performed two experiments for $N < 5$ and $N > 20$, which did not demonstrate an appearance of collective effects.

3. Experimental setup

In our experiments we used Jasmine robots, see Figure 3(a). This microrobot measures $30 \times 30 \times 20 \text{ mm}^3$ and uses two Atmel AVR Mega microcontrollers communicating through an I2C bus.

It has six (60° opening angle) IR channels, used for proximity sensing and for communication, and one IR geometry-perception channel (15° opening angle). The sensing area covers a 360° rose-shaped area with maximal and minimal ranges of 200 and 100 mm, respectively (Kornienko et al., 2005b). The physical communication range can be decreased through a change of sub-modulation frequency. The robot also has a remote control and ZigBee-based robot–host communication. It uses two DC motors with internal gears, and two differentially driven wheels on one axis with a geared motor–wheel coupling. An encoderless odometrical system normalizes the motion of the robot. Jasmine III robots use a 3 V power supply from a Li-Po accumulator with an autonomous work time of 1.25 h. They are capable of autonomous recharging from the power station. More information about these robots, as well as videos of the performed experiments can be found at <http://www.swarmrobot.org>.

The light sensor board uses two identical APDS-9002 sensors and a low-pass filter eliminating 100 Hz AC noise from luminescent light and is placed on top of the robots, see Figure 3(a). The output voltage of the light sensors is fixed by the load resistor and depends on the illumination. The sensor output is directly connected to the ADC inputs of the microcontroller.

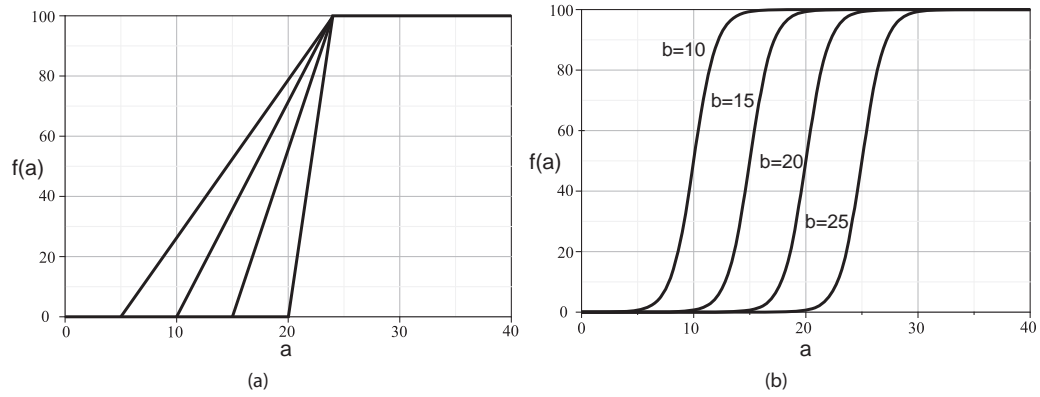


Fig. 2. Two functions $t_w = f(a, b)$ for the control of the waiting function: (a) piecewise linear functions; (b) sigmoid function $t_w = 100/(1 + \exp(b - a))$.

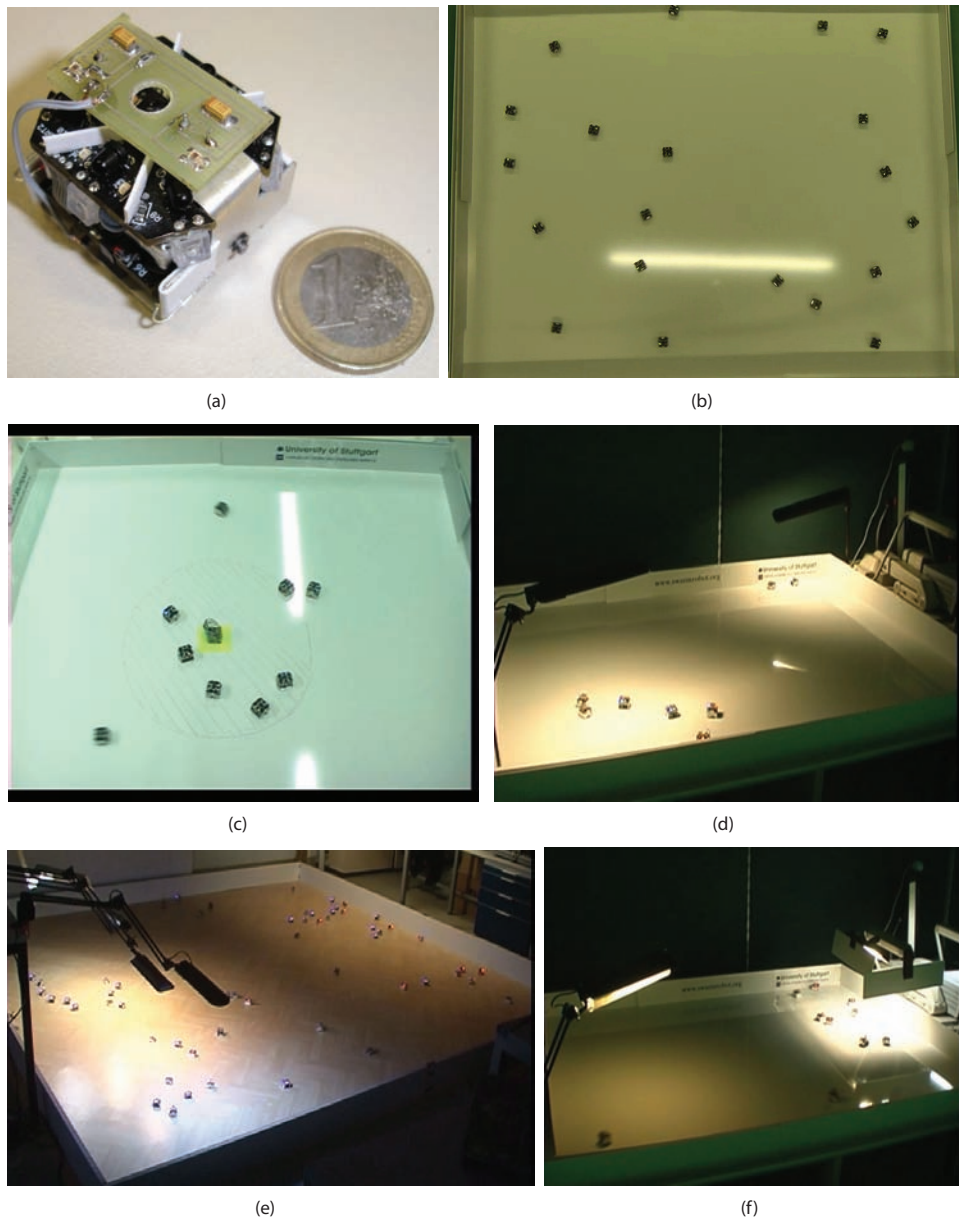


Fig. 3. (a) "Jasmine" microrobot with light sensor board. (b)–(f) Different setups used in the experiments, see Table 2.

Table 2. Overview of the experimental setup, where N is the number of robots, S is the area of the arena and D_{sw} is the swarm density. Experiments are described in the section indicated in the final column: (a) spatial structures in the probability of meetings ; (b) behavior in clusters; (c):i,s decision-making for two light spots with different intensity and sizes; (d) optimal decision-making.

	N	S, m^2	$D_{sw}, N/m^2$	Example	Experiment	Description
1	2; 10; 20	1.4×1.15	1.2; 6.2; 12.4	Figure 3(b)	(a)	Section 2
2	11	0.7×1.15	13.6	Figure 3(c)	(b)	Section 4
3	5; 10; 15; 20; 25	1.4×1.15	3.1; 6.2; 9.3; 12.4; 15.5	Figure 3(d)	(c):i	Section 5
	30; 50; 60	3.0×3.0	3.3; 5.5; 6.6	Figure 3(d)	(c):i	Section 5
4	5; 10; 15; 20; 25	1.4×1.15	3.1; 6.2; 9.3; 12.4; 15.5	Figure 3(d)	(c):s	Section 5
5	4; 6; 8 ;10; 12;	1.4×1.15	2.4; 3.7; 4.9; 6.1; 7.4; 8.6	Figure 3(e)	(d)	Section 6
	14; 16; 20; 45	1.4×1.15	8.6; 9.9; 12.4; 27.9	Figure 3(f)	(d)	Section 6

An overview of the experimental setup is shown in Table 2. The number of robots varies between 2 and 60 with swarm densities between 1.2 and 27.9. This allows the exploration of scalability in different ranges of geometrical and swarm density parameters. For these setups, corresponding simulations in Breve (Klein, 2000) have also been created and used for preliminary tests (Prieto, 2006), see Figure 1(a). The light used in our experiments is produced by luminescent lamps placed in opposite corners of the arena, so as to have equal spatial probability of meetings. In the following we denote the larger/more intense light spot as S_{lg} , labeled “Large”; the smaller/dimmer light spot is denoted as S_{sm} and labeled “Small”. Each experiment is repeated five times. The estimation of the aggregation time is a critical factor, because robots continuously leave and join the group. One approach suggested is to measure the clusters within a fixed time interval (Häbe, 2007), however we encountered large variation of data between trials. In this work we use the approach from Kernbach et al. (2009): the cluster is measured only at such moments as the number of moving robots is minimal, that is, the cluster has a maximal size.

4. Spatial behavior of robots in clusters

The behavior of robots in clusters is an important factor (see e.g. Melhuish et al., 1999), influencing the relationship between t_r and t_w . Moreover, as indicated in Section 2, the geometry of the robot arena creates structures in the probability of robot–robot contacts, which can be used for collective decision-making. Any individual waiting robot can become a seed for a new cluster as soon as other robots collide with it and stop as well in consequence. The largest clusters always appear along the boundaries of the arena, where the probability of meeting is higher (cf. Figure 1(g)–(i)).

The main factor controlling aggregation is the waiting function $f(a)$, see Figure 4 (portion with solid outlines). Robots encountering each other cluster around the energy source, see also (Kernbach et al., 2009). After removing the energy source (for example, a lamp), the robots dis-aggregate. In performing these experiments, we noted that

aggregation is sensitive to the arena and the shape of a cluster.

To explore this effect, we “amplify” the sensitivity of the aggregation process to group-based dynamics in the following way: each robot, before its waiting time is over, senses for neighboring robots and slowly increases the weight of the waiting function $f(a)$. The frequency and the value of updating $f(a)$ determines the dynamics of the clusters. We used two strategies: updating $f(a)$ only once (for experiments in this and in the next section) and updating $f(a)$ at each robot–robot contact (for experiments in Section 6). A short sketch of the algorithm is given in Figure 4 (portion with dashed outlines). In this way, the robots become sensitive to the common strategy of the cluster. Since the approach is not moderated by direct communication, we assess the presence of neighbors by sensing the level of IR noise (Kornienko et al., 2005a). We use modulated IR light for a seed and non-modulated IR light for collision detection; thus, the robots can differentiate between seeds and neighbors.

After detecting a seed, the robots stop moving and sense the level of IR noise. Each time, the robot adopts the current value of $f(a)$ until the waiting time is over and the robot re-starts random movement.

We tested this approach with a group of 11 robots (one robot acting as the cluster seed), see Figure 5(a). At the beginning, the robots are placed in the corner, see Figure 5(a), and the seed, which emits modulated IR light, in the middle of the small $70 \times 115 \text{ cm}^2$ arena. This approach is similar to the experiments with visible light in Section 5. The attraction radius of a seed is marked by a circle on the arena. After 60 seconds, see Figure 5(a)–(f), all of the robots aggregate around the seed. We remove the seed 70 seconds after the start of the experiment, see Figure 5(g). The large cluster splits into two small clusters of three and five robots. The adaptive portion of the algorithm ensures the larger group survives for longer: the group with five robots remains when the group of three robots has disappeared. In the strategy in which each robot becomes a secondary seed after removing the primary seed, this approach can support a decision-making process in which the robots aggregate around a larger cluster (and small clusters disappear).

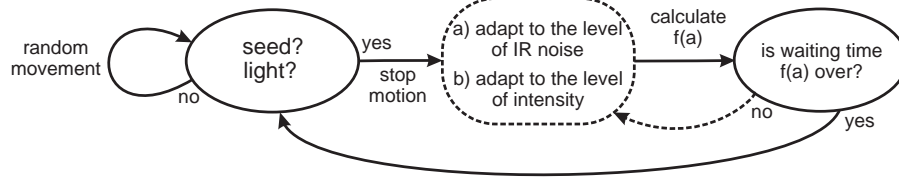


Fig. 4. Sketch of the aggregation algorithm. The dashed box represents the adaptive portion of the algorithm.

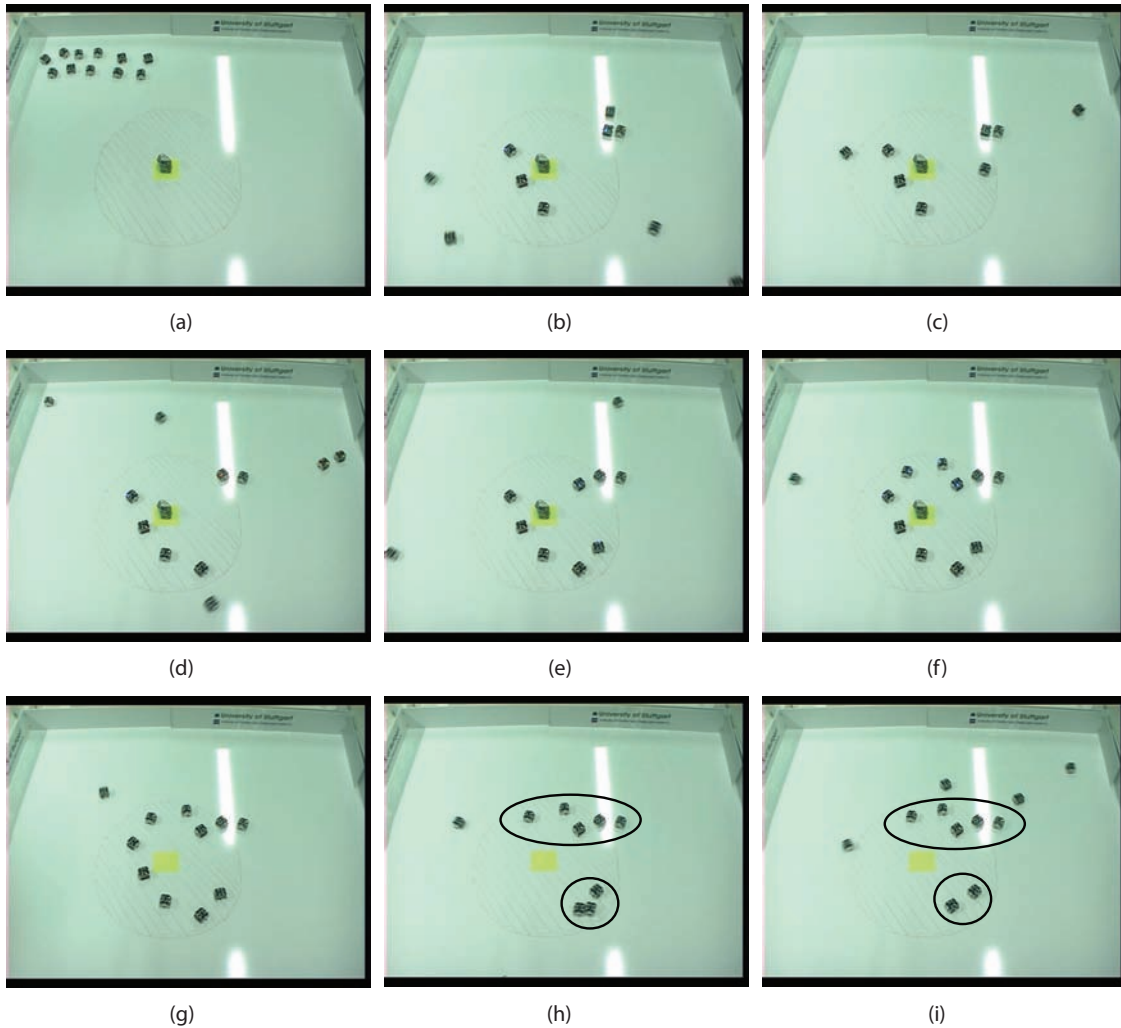


Fig. 5. Experiments with adaptive aggregation, screenshots taken every 10 seconds. (a) Initial state, all robots in the upper left corner, cluster seed placed in the middle of a small arena. The “attraction radius” is indicated by a circle on the arena. (b)–(f) Step-wise aggregation of robots around the seed. (g) Seed removed. (h), (i) Appearance of two groups and their step-wise disaggregation.

To explore the role of spatial conditions, we installed two small obstacles, which reduced the probability of an encounter in the space between the seed and the obstacles, as indicated by the arrows in Figure 6(a).

In this way we created two symmetrical directions for growing the cluster, see Figure 6(a). When removing the seed, we observe symmetry breaking, since the cluster in the upper side is larger and will survive for longer. We performed these experiments several times and observed a bias to the upper side. This can be explained by the fact that

initially all the robots are placed on the upper side, and thus take less time to encounter the seed on the upper side. Thus, using the IR noise as a secondary factor for the waiting function, we can explore structures in the probability of encounter in the arena and use them in the decision-making processes.

To sum up, the algorithm shown in Figure 4 demonstrates aggregation behavior in the presence of a seed and disaggregation behavior some time after removing a seed. We expect more or less comparable results with and without the

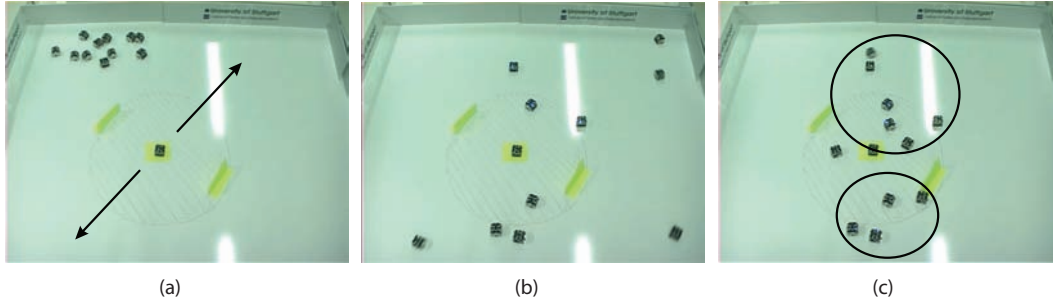


Fig. 6. Spatial structuring of the aggregation including obstacles (made of green paper). (a) Initial state, all robots in the upper left corner, and the cluster seed placed in the middle of a small arena; the direction in which the cluster will grow is indicated by the arrows. The “attraction radius” is indicated by a circle on the arena. (b) Aggregation after 15 seconds. (c) Aggregation after 30 seconds.

adaptive portion in Figure 4 for the experiments with two light sources in the next section. The impact of the adaptation on optimal decision-making is investigated in Section 6. In addition, due to using the IR noise for adaptation of t_w , the robots slow down disaggregation and become to some extent inertial, see Kernbach et al. (2012).

5. Collective decision-making for two light sources of different intensity and size

These experiments use two illuminated lamps. We investigated collective decision-making for: (a) equal size/light intensity of both spots, see Figure 7(a); (b) different intensities, see Figure 7(b); and (c) different sizes, see Figure 10(a). We used the algorithm shown in Figure 4 with and without the adaptive portion. Thus, we can explore the impact of spatial amplification on group strategy.

5.1. Light spots of equal sizes and different intensity

In the first scenario two identical lamps are fixed at a height of 42 cm above opposite corners of the arena. The light intensity, measured by the robot’s sensors, is of values around 150 (values obtained from the ADC). The surface illuminated by the lamps is a quarter of a circle having its center at the corner of the arena, with the radius of $R = 45$ cm. Here N robots cover the area $N\pi R_s^2$, thus each light spot can potentially include

$$N = \frac{R^2}{4R_s^2} \quad (10)$$

robots. For the sensing radius $R_s = 7$ cm each light spot can accommodate $N \approx 10$ robots. Thus, 20 robots represent the lower boundary for reaching a supercritical swarm density. Experimental results for this scenario are shown in Figure 7(c) and in Table 3 for $N = 5, 10, 15, 20$ and 25 robots. We observed a similar distribution of robots between both clusters with essentially no preferred decision.

In the second scenario, two light spots of different intensity are created by lowering one lamp towards the surface,

to a height of 16 cm. The second lamp remains at the same height as in the first scenario. Light sensors record a maximal value of 180 for the stronger spot. The illuminated surface becomes bigger and more oval, with sharper borders, and reaches around 45 and 55 cm away from the corner of the arena. The illuminated area of the stronger spot is almost equal to that of the less intense light in the opposite corner, however with a slightly different geometry. In Figure 7(d) and in Table 3 we show experimental results for this scenario for $N = 5, 10, 15, 20$ and 25 robots. We observed a distribution of 76% versus 12% for five robots between the two light spots. This decision remains noticeable up to a critical swarm size of around 20 robots (for the arena size of 140×115 cm² and the mentioned light spots), above which the decisions are no longer distinguishable as both light spots are filled with robots. The adaptive algorithm slightly increased the number of robots in the stronger spot and reduced the number of robots freely moving between clusters. In Figure 8 we show one particular run of this experiment.

The swarm density varies between 3.1 and 15.5 in these experiments. We observed stable (i.e. repeatable in different experiments) decision-making at $D_{sw} = 3.1; 6.2$. The system becomes saturated at higher densities of $D_{sw} = 9.3–15.5$. To test the scalability of this approach, we performed experiments with 30, 50 and 60 robots in an arena of 9 m², i.e. with $D_{sw1} = 3.3, D_{sw2} = 5.6$ and $D_{sw3} = 6.6$, which correspond to $D_{sw} = 3.1; 6.2$ in the arena of 1.61 m². In these experiments D_{sw} are similar but not the same due to a fixed size of arena in both cases. To generate a stronger light, we used four lamps at a height of 43 cm, and two lamps at a height of 140 cm to create the opposite light spot. In this configuration, each of these spots can cover around 25–30 robots. Several screenshots are shown in Figure 9, the data are collected in Table 3. Since the adaptive algorithm changes the property of the $f(a)$ depending on the environment, the results of the aggregation process with adaptive algorithm become non-comparable. Thus, to be able to compare results of aggregation in two different environments, we used the non-adaptive algorithm for these large-scale experiments.

Table 3. Robots’ distribution as a percentage at the light spots S_{lg} , S_{sm} in the scenarios with equal and different light intensities, using/not using the adaptive portion of the algorithm. Here N is the number of robots. The experiments with 30, 50 and 60 robots are performed in a large 9 m² arena. “Mov.” denotes the percentage of robots still moving after a stable cluster is created. Each experiment is repeated five times, mean values and standard deviations are shown.

N	Equal light spots, % (mean values)						Different light spots, % (mean values)					
	No adaptive part			With adapt. part			No adapt. part			With adapt. part		
	S_{lg}	S_{sm}	Mov.	S_{lg}	S_{sm}	Mov.	S_{lg}	S_{sm}	Mov.	S_{lg}	S_{sm}	Mov.
5	48.0	48.0	4.0	44.0	48.0	8.0	76.0	12.0	12.0	80.0	12.0	8.0
10	48.0	42.0	10.0	48.0	50.0	2.0	76.0	18.0	6.0	82.0	12.0	6.0
15	44.0	45.0	11.0	48.0	48.0	4.0	49.0	28.0	23.0	56.0	40.0	4.0
20	47.0	45.0	8.0	47.0	47.0	6.0	46.0	44.0	10.0	45.0	47.0	8.0
25	38.0	38.0	23.0	44.0	38.0	18.0	40.0	38.0	22.0	42.0	40.0	18.0
30	—	—	—	—	—	—	64.0	15.0	21.0	—	—	—
50	—	—	—	—	—	—	42.0	23.0	35.0	—	—	—
60	—	—	—	—	—	—	48.0	33.0	19.0	—	—	—

N	Equal light spots, % (StdDev)						Different light spots, % (StdDev)					
	No adaptive part			With adapt. part			No adapt. part			With adapt. part		
	S_{lg}	S_{sm}	Mov.	S_{lg}	S_{sm}	Mov.	S_{lg}	S_{sm}	Mov.	S_{lg}	S_{sm}	Mov.
5	10.9	10.9	8.9	8.9	10.9	10.9	16.7	17.8	17.8	14.1	10.9	17.8
10	14.8	19.2	12.2	8.3	7.0	4.4	11.4	8.3	5.4	8.3	10.9	5.4
15	5.9	5.5	5.9	9.8	8.6	5.9	7.6	10.9	14.6	7.6	10.9	14.6
20	2.7	3.5	2.7	7.5	4.4	4.1	4.1	4.1	6.1	3.5	6.7	7.5
25	6.6	4.5	9.5	4.0	6.0	9.2	4.8	4.5	7.2	4.5	6.3	9.2
30	—	—	—	—	—	—	11.9	5.0	9.3	—	—	—
50	—	—	—	—	—	—	3.1	6.1	7.8	—	—	—
60	—	—	—	—	—	—	4.3	3.9	5.9	—	—	—

We again observed stable collective decisions for the stronger light spot (64% versus 15%, 42% versus 23% and 48% versus 33%). The aggregation time varies between 4 and 7 min (1.5–3 min in the small arena). We performed a Mann–Whitney U -test for all aggregation trials in the cases of the different light spots, which delivers $U = 0$ for $Z = -2.6$ and $p < 0.009$ two-tailed for $D_{sw} \leq 6.6$.

5.2. Light spots of equal intensity and different sizes

In this experiment we created two light spots of equal intensity but different sizes. The results are collected in Figure 10(a) and Table 4. Both lamps are installed at a height of 42 cm, but the lamp at the bottom of the arena is moved 30 cm into the arena. Thus, the light spot at the bottom is 75% larger than the light spot at the top of the arena. The different size of the spots is a decisive factor for small swarm sizes ($N < 15$), because a larger number of robots can be accommodated under the large spot. For $N = 5$ (or 10) we observed e.g. 84% versus 8% (70% versus 10%) decisions with a small variance from the mean value, see Figure 10(b). In Figures 10(c)–10(h) we demonstrate one particular run with eight robots, where we observe a 100% versus 0% collective decision. To make this approach

clearer, all of the robots in the initial setup are placed first in the smaller light spot, see Figure 10(c).

Eventually, most of the robots aggregate under the large spot. Since the intensities of both spots are the same, this decision is influenced only by the spatial probability of encountering each other. We note that the 100% versus 0% decision very seldom occurs, because robots at the boundary of a cluster spontaneously disaggregate and run in the arena. When several robots meet under a smaller light spot, they create a cluster. We observe this situation when increasing the swarm density. The Mann–Whitney U -test delivers $U = 0$ for $Z = -2.6$ and $p < 0.009$ two-tailed for all cases below the critical swarm density $D_{sw} \leq 6.6$.

To conclude this section, we observed stable decision-making behavior for different light spots. The decision behavior is stable and highly reproducible over many experiments, as long as the swarm density remains below the critical level described by (10). The behavior is very scalable in terms of different swarm densities, as well as for the same swarm density but using different numbers of robots and different arena sizes. The control experiment with equal light spots did not demonstrate any essential decisions. The setup with different spot sizes demonstrated more evident decisions (i.e. larger difference of means for small and large light spots) than the setup with different light intensities. However, this reflects only the chosen relationship

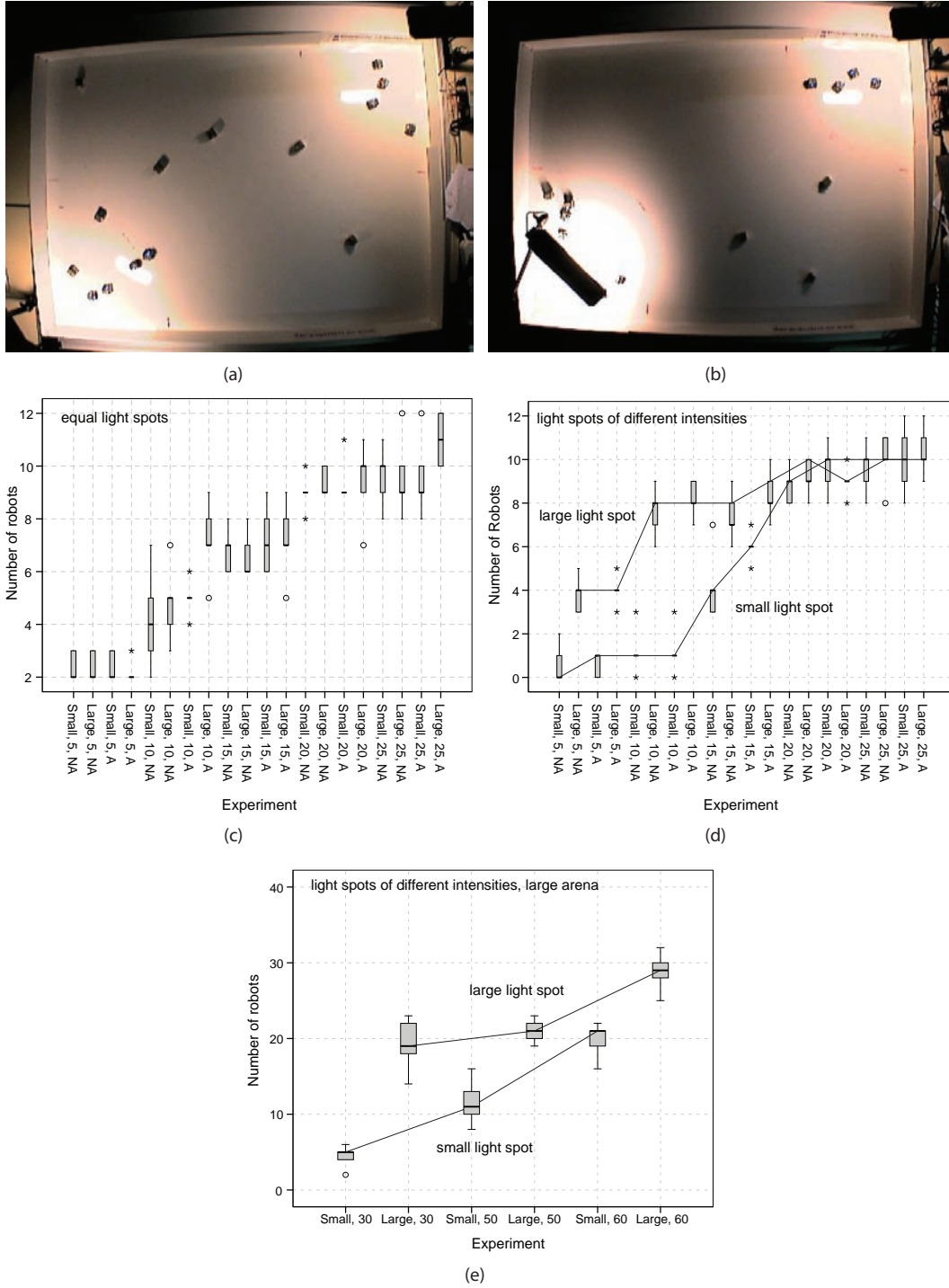


Fig. 7. Experiments with two light spots of (a) equal size and intensity and (b) different intensities. (c)–(e) Plots demonstrating the number of robots aggregated under each light spot. “A” denotes adaptive algorithm, “NA” denotes non-adaptive algorithm, “Small” and “Large” correspond to light spots with, respectively, equal and different intensity. The number represents the total number of robots used in the experiment. For instance, the label “Small, 10, A” means the number of robots aggregated in the small light spot in the experiment with 10 robots by using the adaptive algorithm. In (c)–(e), circles are used for outliers and stars for extreme outliers.

between t_w and t_r in these experiments. Generally, this can be changed, for example by making the waiting time in $f(a)$ shorter or longer. The adaptive algorithm generates more

stable clusters for stronger/larger light spots and reduces the number of robots freely moving between clusters, especially in the case of small/large light spots, see Figure 10(b).

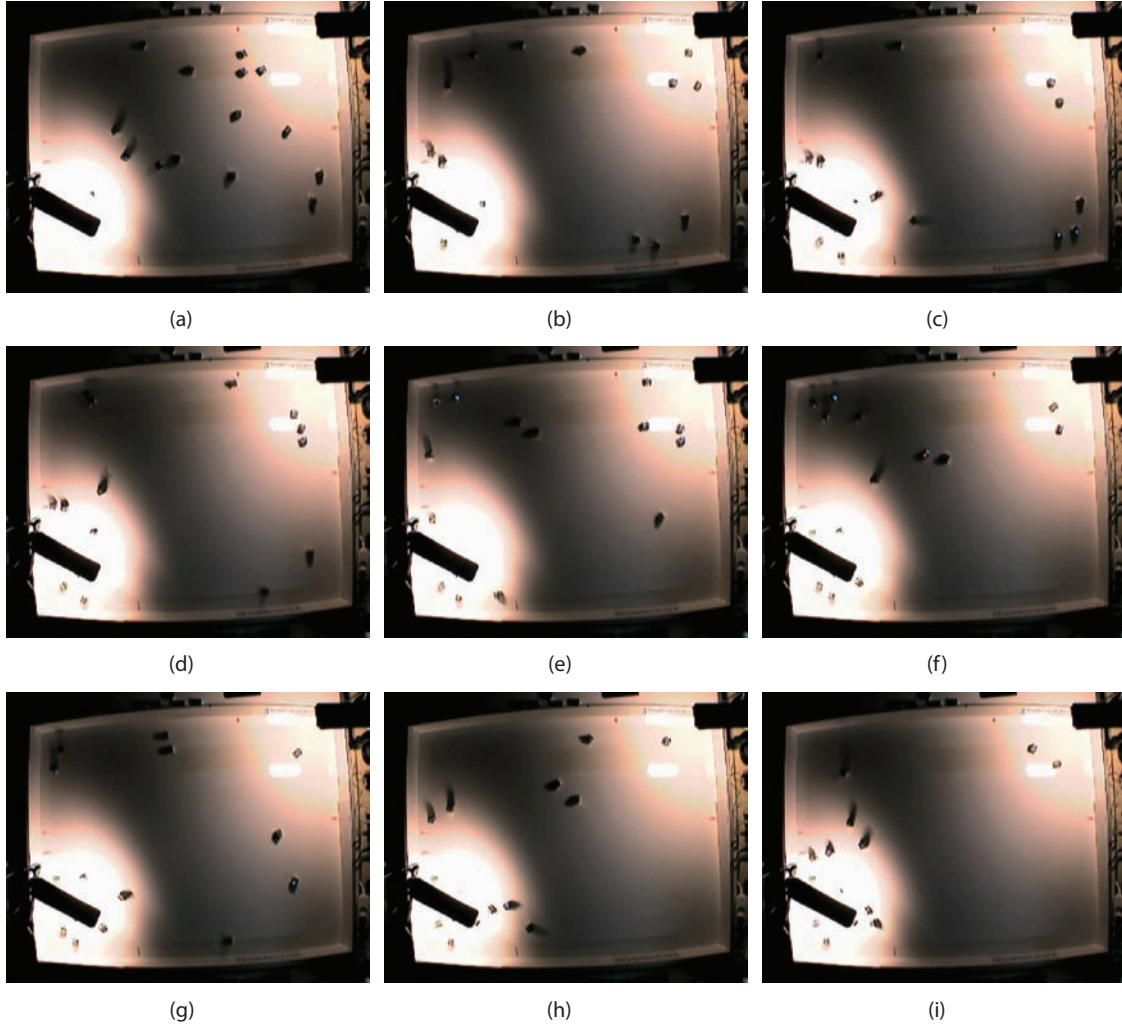


Fig. 8. One run of the experiment with two light spots of different intensity, images taken at 10 second intervals.

Table 4. Robot distribution as a percentage at the light spots S_{lg} , S_{sm} in the scenarios with equal and with different sizes of light spots using/not using the adaptive portion of the algorithm, N is number of robots. “Mov.” means the percentage of robots still moving. Each experiment is repeated five times, mean values and standard deviations are shown.

N	Mean values, %						StdDev, %					
	No adaptive portion			With adapt. part			No adaptive portion			With adapt. part		
	S_{lg}	S_{sm}	Mov.	S_{lg}	S_{sm}	Mov.	S_{lg}	S_{sm}	Mov.	S_{lg}	S_{sm}	Mov.
5	84.0	8.0	8.0	88.0	4.0	8.0	16.7	17.8	10.9	10.9	8.9	10.9
10	70.0	10.0	20.0	68.0	14.0	18.0	10.0	14.1	14.1	16.4	8.9	10.9
15	55.0	24.0	21.0	56.0	25.0	19.0	8.6	12.1	15.2	11.1	5.5	8.6
20	40.0	19.0	41.0	50.0	21.0	29.0	7.9	11.9	8.2	9.3	8.9	13.4
25	38.0	26.0	36.0	39.0	29.0	32.0	10.4	9.6	14.9	7.6	8.1	11.3

6. Experiments with optimal collective decision-making

Experiments from Section 5 were performed with two lamps emitting light at the same time. Robots can collectively decide in favor of more intense light or larger light spots. Owing to the nature of the algorithm, robots on the

boundaries of a cluster disaggregate and move randomly in the arena until they encounter a cluster, when they stop again. This can be understood as an exploratory behavior, in which a swarm continuously monitors its environment. In Figure 11 we plot the number of such moving robots for all three experiments from the previous section.

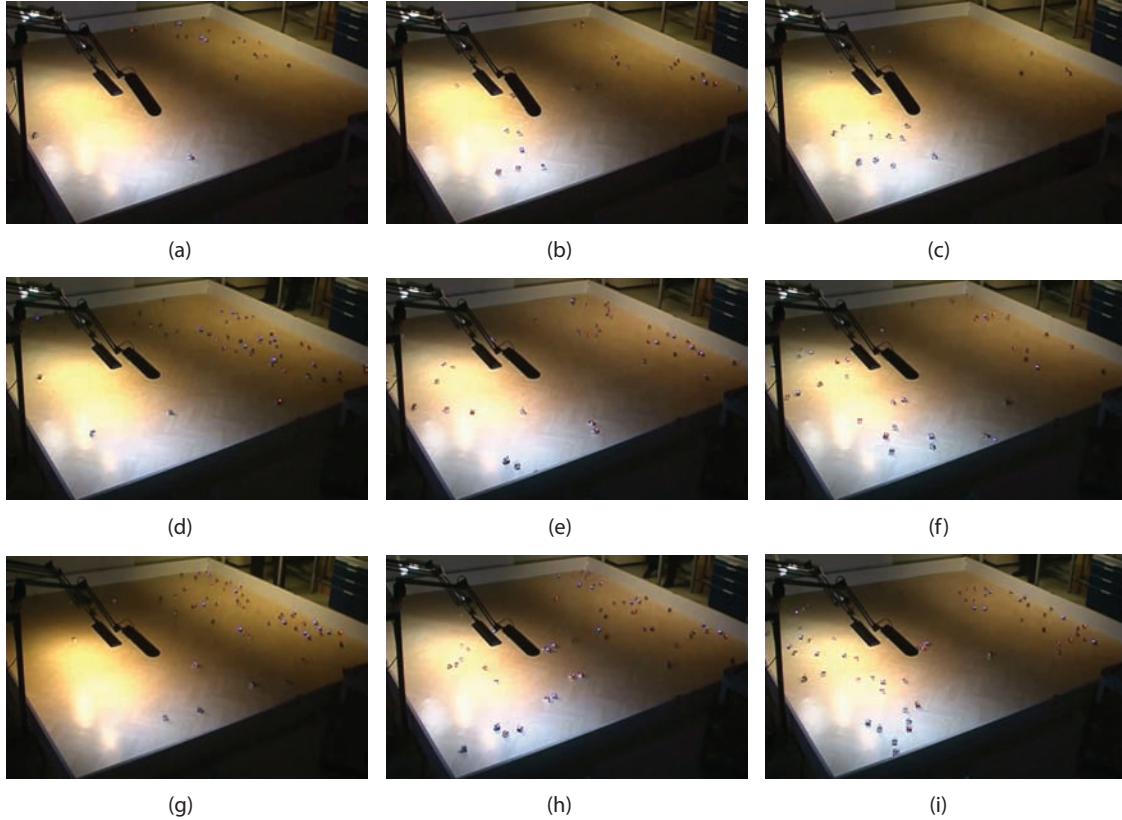


Fig. 9. Experiment with light spots of different intensity in the large arena. (a), (d), (g) Initial setup with 30, 50 and 60 robots; (b), (e), (h) after 2 minutes; (c), (f), (i) after approximately 5 minutes.

We observe a general trend of an increasing number of free-moving robots with swarm density. When such disaggregated robots meet each other under a weaker or smaller light spot, they can create a new cluster. This behavior can be observed even when the swarm density is low, that is, there is still enough room under the stronger/larger lamps. This is why, in the decision-making behavior, we find a small number of robots in the weaker/smaller light spot. When we consider this situation from the energetic viewpoint, such behavior in the swarm is not optimal because it reduces the total energy income.

To optimize the energy income, we extend the ideas from Section 4, where robots in a cluster adapt the waiting time t_w according to the size of the cluster. As we observed in Sections 4 and 5 this small modification allows for exploration of symmetry-breaking and improving performance. In a similar way, robots can adapt waiting time to the light intensity of the cluster. In the algorithm shown in Figure 4, a robot, when encountering another robot, measures light intensity and calculates the waiting function $f(a)$. When the value of light is low, see Figure 12(a), the waiting time t_w is zero. Then the robots slightly shift the waiting function, as shown in Figure 12(b).

When t_w is still equal to zero, a robot moves away. When the robots meet each other under the light, $f(a)$ is shifted step-by-step left-wise. Thus, each time they meet

each other, the robots adapt $f(a)$ to the light conditions sensed. The adaptation of $f(a)$ is bounded by a_{\min} and a_{\max} , which define the minimal intensity level acceptable for building clusters and preventing the saturation of $f(a)$ by very intense light.

Depending on the swarm density, this behavior creates two effects. For low swarm densities, all of the robots that visited an energy-intensive cluster will not aggregate under less energy-intense light. This strategy is in fact a greedy search approach for maximizing the value of the total energy income of a swarm. When all of the robots in the arena can be covered by one of the light spots, we can expect a strong collective decision, 100% versus 0%. In other words the whole swarm decides on one of the available targets. For a higher swarm density, when all of the robots on the arena cannot be covered by one of the light spots, we expect a division of labor to emerge. The cluster at the most intense light will be fully occupied by robots, and all of the remaining robots will be collected under the weaker light. Neither group will be able to exchange robots.

To demonstrate this approach, the degree of light intensity in both spots should not overlap. Figures 8, 10 show there is a small region where the stronger light spot overlaps with the weaker spot. To remove this overlapping, we changed the geometry of the stronger light spot, making its boundary sharp, see Figure 13(c). We first switched on

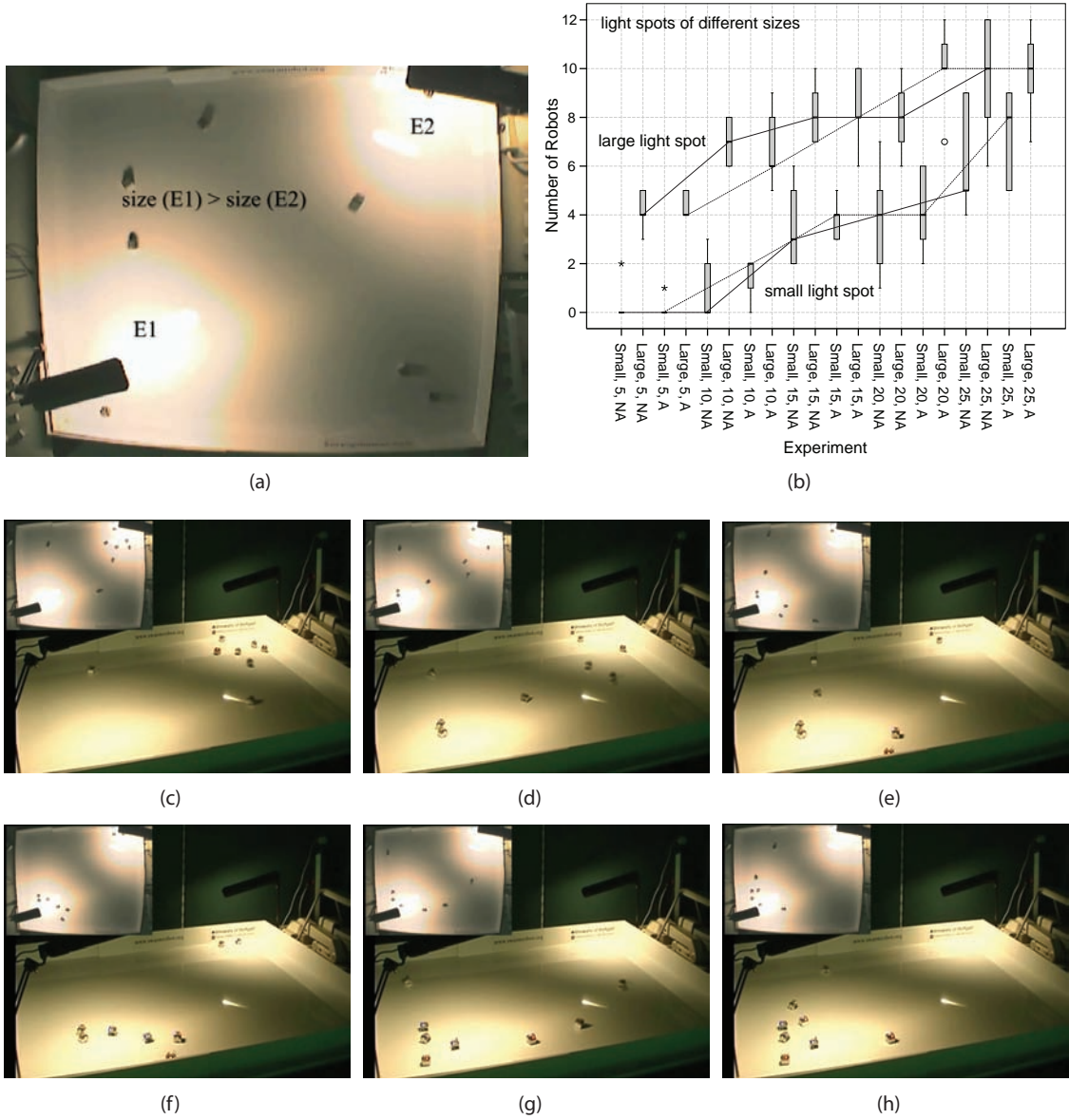


Fig. 10. Experiment with light spots of different size. (a) Top-down image of the arena. (b) The number of robots aggregated under light spots of different sizes. For example, the Mann–Whitney U -test delivers the values for $N = 10$ (non-adaptive algorithm) the medians for small/large light spot 0/7 robots with $U = 0$, $Z = -2.66$, $p < 0.05$ two-tailed and for $N = 25$ the median 5/10 robots with $U = 4$, $Z = -1.792$, $p < 0.095$ two-tailed. (c)–(h) One run of the experiment, showing top-down and sideways views (30-second interval between images).

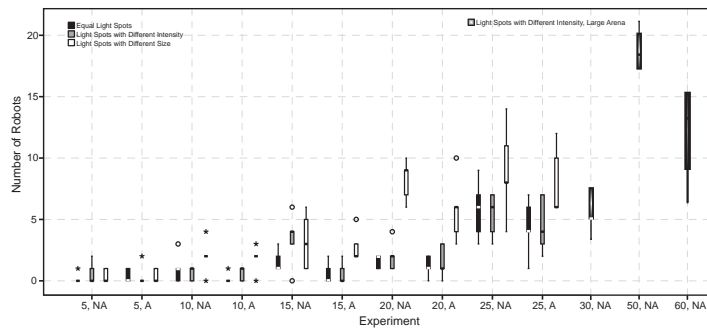


Fig. 11. Number of robots moving between clusters in all experiments from Section 5.

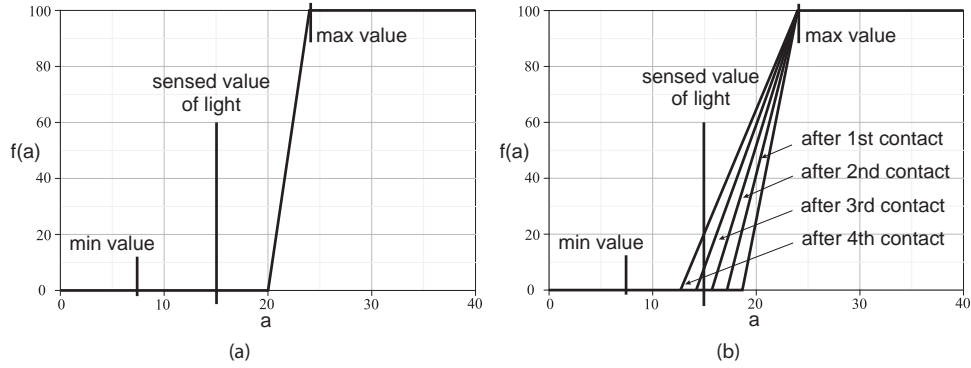


Fig. 12. Step-wise modification of the waiting time $f(a)$ to light conditions sensed.

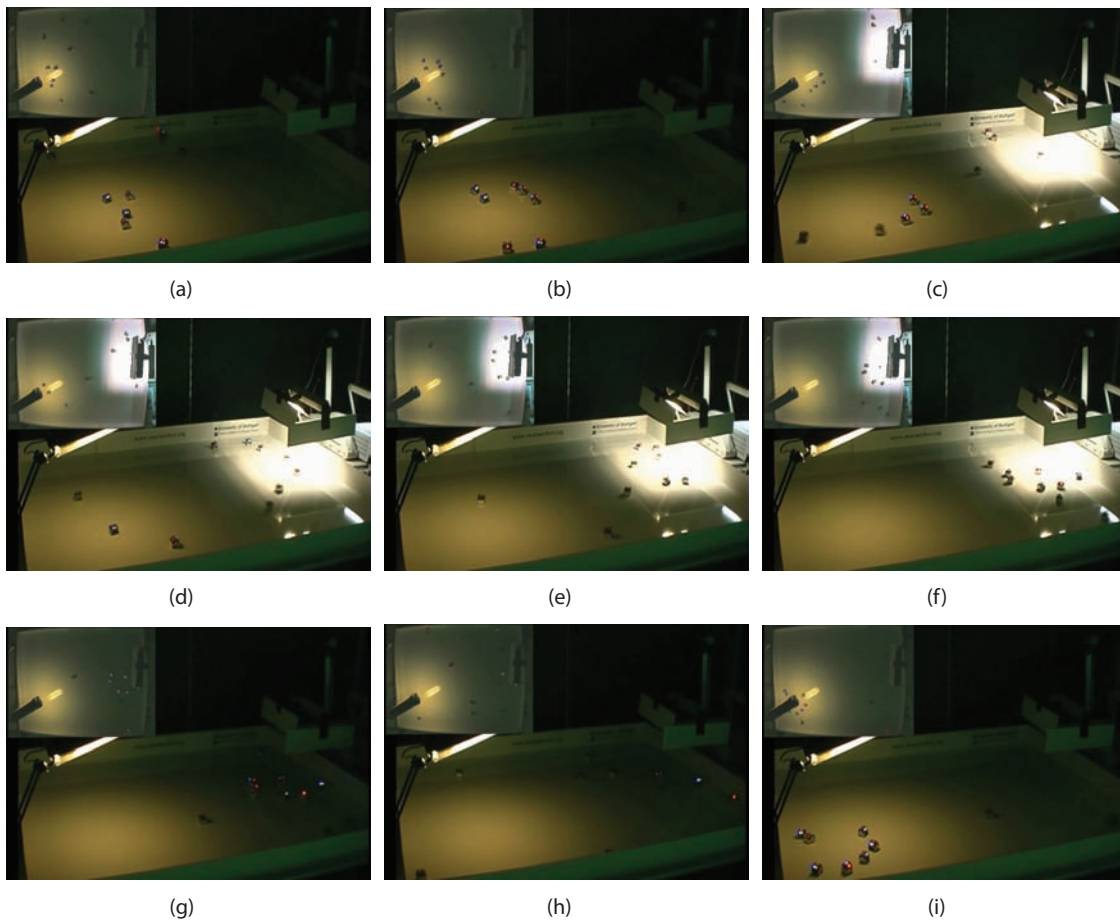


Fig. 13. Experiment with light spots of different size. (a) Top-down image of the arena; (b) percentage of robots aggregating in each light spot; (c)–(h) one run of the experiment with top-down and sideways views (30-second time interval between (c) and (h) and 3-minute time interval between images (h) and (i)).

the weaker light spot and let the robots adapt to its intensity, see Figure 13(a) and (b). Then the intense light was switched on and we observed that within 1.5–2 minutes all of the robots aggregated within this spot. For swarm sizes between 6 and 12 robots, no robots were observed aggregating under the weaker light. After ~ 3.5 minutes we switched off the intense light spot, see Figure 13(g) and the robots aggregated again under the weaker light.

The strong light spot can only cover about nine robots, however stable 100% versus 0% behavior was observed slightly beyond this number. We performed experiments varying the number of robots between 6 and 20. Stable 100% versus 0% decisions were observed with up to 12 robots. Above this number, the robots created a second cluster, as shown in Figure 14. In the experiments, we observed no exchange of robots between clusters, especially at higher

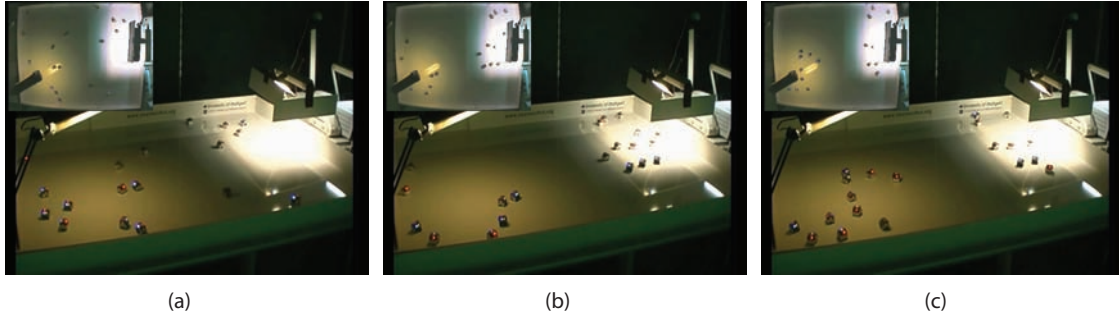


Fig. 14. Experiment: division of labor based on intensity of light spots. Robots from a stronger light spot never halt under the weaker light (40-second time interval between images).

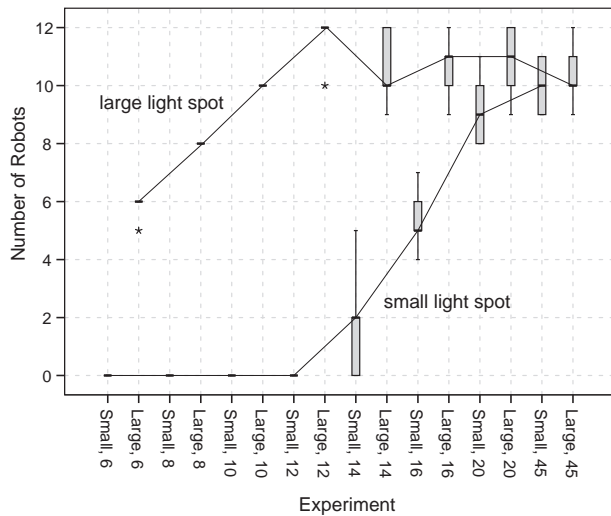


Fig. 15. Number of robots aggregated under different light spots.

swarm densities. It must be noted that the robots still dis-aggregate from a cluster but they always return to the same cluster. Several images from these experiments are shown in Figure 14. The parameters of the experiments are collected in Table 5 and in Figure 15.

This “emergent specialization” of robots in both clusters points to a mechanism for the division of labor, where the initial placement is decided by a random choice but then embodied in the parameters of the waiting function $f(a)$. A comparable mechanism for the emergence of division of labor has been suggested for insect societies (Theraulaz et al., 1998). Such an approach can be used in more general mechanisms for generating weakly emergent collective behavior (Kornienko et al., 2004a). When the number of robots was more than 20, we observed robots beginning to move between clusters.

As mentioned in Section 2.2, the collective effects appear when the swarm density satisfies boundary conditions for subcritical and supercritical swarm densities. We performed two experiments with $N = 4$ and $N = 45$ robots, see Figure 16(a) and (b). In neither case are there any observable collective phenomena.

7. Discussion of results and conclusion

In summary, we would like to discuss several open issues. First, the primary motivation for the experiments performed originated in the mesoscopic domain of microrobotics. Autonomous systems between 10^{-3} and 10^{-4} m possess a degree of programmability, for example it is possible to control repulsion or attraction between elements through hydrophilic/hydrophobic properties, such as electrostatic forces or molecular effects such as DNA hybridization (European Union, 2006-2009). We simulated these effects by simply stopping the motion of the robot. Mesoscopic systems can be made sensitive to light in terms of electrochemical reactions or photovoltaic effects (Kobayashi et al., 1984). It is also possible to connect, in a purely reactive way, the light sensitivity of mesoscopic elements to their attracting or repelling properties. In the robots, we used SMD light sensors and a microcontroller to calculate a simple piecewise linear or sigmoid function for the waiting time. The robots use no direct peer-to-peer or global communication and do not store light values for digital processing. Thus, we approximated the minimalistic properties of mesoscopic systems with larger robots. It is clear that multiple fluidic, surface or random phenomena at this level cannot be reproduced at a larger scale. However, the chief intention was to demonstrate that elements possessing the “intelligence of dust” at the micro-level can possess some simple forms of collective intelligence at the macro-level.

We argued that a simple form of macroscopic intelligence can be recognized, in terms of rational decision-making and some adaptive or optimizing behavior. At the microscopic level, the robots do not perceive the whole arena and know neither the choices nor the behavior of the whole group. We demonstrated that a swarm of robots can collectively decide to locate in an energy-rich place in both the cases of stronger illumination and a larger area of illumination. Collective decision-making can also explore a symmetry-breaking effect. In particular, we demonstrate the probability that the robot-to-robot contacts possess spatial structures. Their characteristics are determined by the collision avoidance behavior of the robots, correlated random motion (Kareiva and Shigesada, 1983) or even by the initial placing of the robots. In creating a symmetry-breaking

Table 5. Several parameters of the experiments. Here N is the total number of robots taking part in the experiment; S_i is the average percentage of robots aggregated under the first, intense, lamp; S_d is the average percentage of robots aggregated under the second, dim, lamp; t is the time required to adapt from the Intense to dim lamp and vice versa. Since robots join and leave clusters, S_i and S_d are calculated when the corresponding cluster becomes stable (no moving robots) and t_{I-D} , t_{D-I} are measured as the time between switching the corresponding lamp on and off and the creation of the first stable cluster under the opposite lamp.

Mean values					StdDev			
N	S_i (%)	S_d (%)	t_{I-D} (s)	t_{D-I} (s)	S_i (%)	S_d (%)	t_{I-D} (s)	t_{D-I} (s)
4	0	0	—	—	0	0	—	—
6	97	0	251	199	7.5	0	18.8	19
8	100	0	220	184	0	0	15.8	8.2
10	100	0	203	167	0	0	14.8	12
12	95	0	172	139	7.5	0	16.6	14
14	76	13	144	117	9.6	15	11.4	12
16	66	34	125	105	7.1	7	10	11
20	54	46	97	94	6.5	7	12	9.6
45	23	22	—	—	2.5	2	—	—

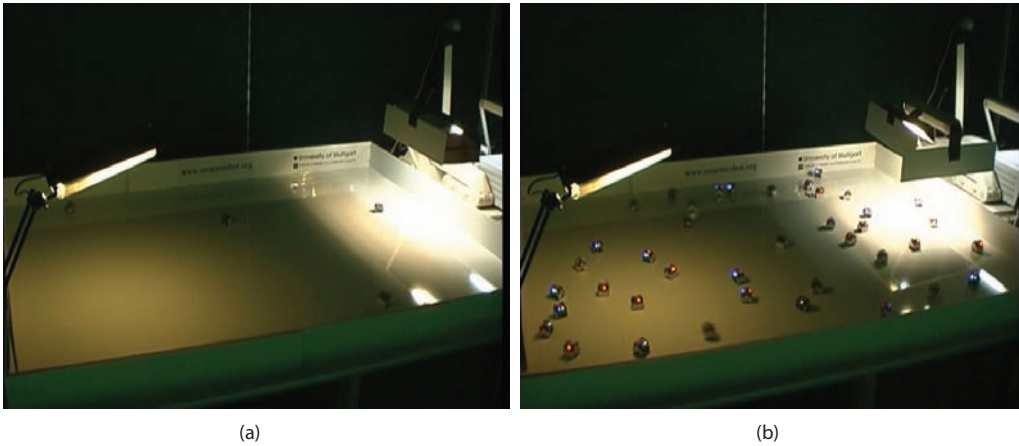


Fig. 16. Effect of (a) subcritical swarm density (4 robots) and (b) supercritical swarm density (45 robots). In neither case are there any observable collective phenomena.

condition, the robots can exploit these structures in their decision-making processes.

Collective decision-making can possess an adaptive functionality, in terms of greedy optimization of the total energy income. The price paid for this adaptive collective behavior is the ability to change one parameter of the waiting function $f(a)$. This requires more functionality from the mesoscopic system and raises the question of the simple programmability of such systems. When these technological difficulties can be solved, we will observe adaptive collective properties on the macroscopic level.

We observed the value $\frac{2\sqrt{2}R_s v}{S}$ several times in kinetic interactions between microrobots (Kernbach, 2008, 2011; Kernbach et al., 2012). It seems that the radius R of either the sensing R_s or communication range R_c , the speed of motion v and the swarm area S represent a fundamental meaning for kinetic interactions, which can be denoted as the swarm reactivity constant φ

$$\varphi = \frac{2\sqrt{2}Rv}{S}. \quad (11)$$

The value φ has a physical dimension $1/t$ and demonstrates internal inertness of the swarm, which refers to the speed with which the swarm is able to react to external stimuli in the context of spatial interactions.

We encountered several problems in performing the robot experiments. The number of trials is low (5 per experiment) and we foresee difficulties in increasing them to a level essential for unbiased statistical significance (for example, 30 trials per experiment). The problems are of a technical character related to maintaining a large number of robots, and to variations in the behavior of individual robots. These problems are often mentioned in connection with swarm robotic experiments (Kornienko et al., 2004b; Fu, 2005; Kernbach et al., 2009). In contrast, experimentation with social insects is not hampered by such problems. Large colonies can be maintained at low cost, thus making these agents a virtually unlimited factor in experimental set-ups. Albeit not deliberately configurable like robots, individuals have a wide range of behavioral variability which can be exploited to approximate the robots' primitive programmability. For instance, we observed different forms of individual locomotion

behavior in honeybees, which can be regarded as a biological equivalent to different implementations of the waiting function in robots. By deliberately picking individuals with specific traits, a honeybee swarm can be composed and prepared for specific tasks, just like robot swarms are by tweaking their internal parameters.

In the future, we would like to explore our approaches with a larger macroscopic (Kernbach et al., 2008) and a smaller mesoscopic system, consisting of functionalized components with programmable surfaces. In addition, we expect interesting results from the comparison of experiments with robots and honeybees and to gain better knowledge about the rules by which the different forms of embodiment relate a primitive fundamental program to the ultimate (emergent) swarm behavior. In this way, bio-inspired robotic research will provide valuable feedback for biological research. It might even be possible to draw conclusions on the fundamental individual mechanisms that underlie the social behavior of living organisms by reproducing such a swarm with robots and manipulating the parameters that determine their strategy. This approach also might enable biologists to better assess the benefits and costs of individual variability and the adaptive properties of the resultant swarm heterogeneity. As of yet, this is still an open question in biology. The sum of these approaches would allow a deeper understanding of the problems in, and approaches for, creating collective intelligence from limited elements.

Funding

S Kernbach and O Kernbach are supported by the EU-IST FET project “I-SWARM” (grant number 507006), EU-IST FET project “SYMBRION” (grant number 216342) and EU-ICT project “REPLICATOR” (grant number 216240). R Thenius, G Radspieler, T Kimura and T Schmickl are supported by EU-IST FET project “I-SWARM” (grant number 507006) and by the FWF research grants “Temperature-induced aggregation of young honeybees” (grant number P19478-B16) and “REBODIMENT - Bienenemulierende Roboterschwärme erkunden 2-dimensionale Temperaturfelder” (grant number P23943-N13).

Acknowledgement

We wish to thank all members of the project for fruitful discussions.

References

- Ame JM, Rivault C and Deneubourg JL (2004) Cockroach aggregation based on strain odour recognition. *Animal Behaviour* 68: 793–801.
- Bellomo EG, Wyrsta MD, Pakstis L, Pochan DJ and Deming TJ (2004) Stimuli-responsive polypeptide vesicles by conformation-specific assembly. *Nature Materials* 3: 244–248.
- Bodi M, Thenius R, Schmickl T and Crailsheim K (2009) Robustness of two interacting robot swarms using the BEECLUST algorithm. In: Troch I and Breitenacker F (eds), *MATHMOD 2009 - 6th Vienna International Conference on Mathematical Modelling*.
- Bodi M, Thenius R, Schmickl T and Crailsheim K (2010) How two cooperating robot swarms are affected by two conflictive aggregation spots. In: *10th European Conference on Artificial Life (ECAL'09) (Lecture Notes in Computer Science, vol II.)*. New York: Springer.
- Bonabeau E, Dorigo M and Theraulaz G (1999) *Swarm Intelligence - From Natural to Artificial Systems*. Oxford: Oxford University Press.
- Bonabeau E, Theraulaz G, Deneubourg JL, Aron S and Camazine S (1997) Self-organization in social insects. *Trends in Ecology and Evolution* 12: 188–193. DOI: 10.1016/S0169-5347(97)01048-3.
- Bonabeau E, Theraulaz G, Fourcassi V and Deneubourg JL (1998) *The Phase-ordering Kinetics of Cemetery Organization in Ants*. Technical Report 98-01008, Santa Fe Institute.
- Byers JA (2001) Correlated random walk equations of animal dispersal resolved by simulation. *Ecology* 82: 1680–1690.
- Camazine S, Deneubourg JL, Franks NR, Sneyd J, Theraulaz G and Bonabeau E (2001) *Self-Organization in Biological Systems*. Princeton, NJ: Princeton University Press.
- Camazine S and Sneyd J (1991) A model of collective nectar source selection by honey bees: Self-organization through simple rules. *Journal of Theoretical Biology* 149: 547–571.
- Camazine S, Sneyd J, Jenkins MJ and Murray JD (1990) A mathematical model of self-organized pattern formation on the combs of honeybee colonies. *Journal of Theoretical Biology* 147: 553–571.
- Caruso F (2001) Nanoengineering of Particle Surfaces. *Advanced Materials* 13(1): 11–22.
- Crailsheim K, Eggenreich U, Ressi R and Szolderits M (1999) Temperature preference of honeybee drones (Hymenoptera: Apidae). *Entomologia Generalis* 24(1): 37–47.
- Deneubourg JL, Aron S, Goss S, and Pasteels JM (1990a) The self-organizing exploratory pattern of the argentine ant. *Journal of Insect Behavior* 3: 159–168.
- Deneubourg JL, Gregoire JC and Fort EL (1990b) Kinetics of larval gregarious behavior in the bark beetle *Dendroctonus micans* (Coleoptera: Scolytidae). *Journal of Insect Behavior* 3: 169–182.
- Deneubourg JL, Lioni A and Detrain C (2002) Dynamics of aggregation and emergence of cooperation. *Biological Bulletin* 202: 262–267.
- Depickere S, Fresneau D and Deneubourg JL (2004) Dynamics of aggregation in *Lasius niger* (formicidae): influence of polyethism. *Insectes Sociaux* 51(1): 81–90.
- Dorigo M, Bonabeau E and Theraulaz G (2000) Ant algorithms and stigmergy. *Future Generation Computer Systems* 16: 851–871.
- Fellermann H, Rasmussen S, Ziock HJ and Solé RV (2007) Life cycle of a minimal protocell—a dissipative particle dynamics study. *Artificial Life* 13: 319–345. DOI: 10.1162/artl.2007.13.4.319.
- European Union (2006–2009) *GOLEM: Bio-inspired Assembly Process for Mesoscale Products and Systems*. EU Project NMP-2004-3.4.1.2-1.
- Fu Z (2005) *Swarm-based Computation and Spatial Decision Making*. Master Thesis, University of Stuttgart.
- Häbe D (2007) *Bio-inspired Approach Towards Collective Decision Making in Robotic Swarms*. Diploma Thesis, University of Stuttgart.

- Halpern J and Mosesi Y (1990) Knowledge and common knowledge in a distributed environment. *Journal of the Association for Computer Machinery* 37: 549–587.
- Heran H (1952) Untersuchungen über den temperatursinn der honigbiene (*Apis mellifica*) unter besonderer berücksichtigung der wahrnehmung von strahlungswärme. *Journal of Comparative Physiology A: Neuroethology, Sensory, Neural, and Behavioral Physiology* 34: 179–207.
- Jeanson R, Rivault C, Deneubourg JL, et al. (2004) Self-organized aggregation in cockroaches. *Animal Behaviour* 69: 169–180.
- Johnson NL, Kemp AW and Kotz S (2005) *Univariate Discrete Distributions*. New York: John Wiley & Sons.
- Kareiva PM and Shigesada N (1983) Analyzing Insect Movement as a Correlated Random Walk. *Oecologia* 56: 234–238. DOI: 10.2307/4216888.
- Kernbach S (2008) *Structural Self-organization in Multi-Agents and Multi-Robotic Systems*. Berlin: Logos Verlag.
- Kernbach S (2011) Improving the scalability of collective systems. In: Kernbach S (ed.), *Handbook of Collective Robotics: Fundamentals and Challenges*. Singapore: Pan Stanford Publishing, pp. 225–256.
- Kernbach S (ed.) (2012) *Handbook of Collective Robotics: Fundamentals and Challenges*. Singapore: Pan Stanford Publishing.
- Kernbach S and Kernbach O (2011) Collective energy homeostasis in a large-scale micro-robotic swarm. *Robotics and Autonomous Systems* 59: 1090–1101. DOI: 10.1016/j.robot.2011.08.001.
- Kernbach S, Nepomnyashchikh V, Kancheva T and Kernbach O (2012) Specialization and generalization of robotic behavior in swarm energy foraging. *Mathematical and Computer Modelling of Dynamical Systems* 18: 131–152. DOI: 10.1080/13873954.2011.601421.
- Kernbach S, Ricotti L, Liedke J, Corradi P and Rothermel M (2008) Study of macroscopic morphological features of symbiotic robotic organisms. In: *Proceedings of the Workshop on Self-reconfigurable Robots (IROS08)*, Nice, pp. 18–25.
- Kernbach S, Thenius R, Kernbach O and Schmickl T (2009) Re-embodiment of honeybee aggregation behavior in artificial micro-robotic system. *Adaptive Behavior* 17: 237–259.
- Kimura T, Ohashi M, Okada R and Ikeno H (2011) A new approach for the simultaneous tracking of multiple honeybees for analysis of hive behavior. *Apidologie* 42: 607–617.
- Klein J (2000) *Breve Project*. <http://www.spiderland.org/breve/>.
- Kobayashi T, Yoneyama H and Tamura H (1984) Electrochemical reactions concerned with electrochromism of polyaniline film-coated electrodes. *Journal of Electroanalytical Chemistry and Interfacial Electrochemistry* 177: 281–291. DOI: 10.1016/0022-0728(84)80229-6.
- Kornienko S, Kornienko O and Levi P (2003) Flexible manufacturing process planning based on the multi-agent technology. In: *Proceedings of the 21st IASTED International Conference on AI and Applications (AIA '2003)*, Innsbruck, Austria, pp. 156–161.
- Kornienko S, Kornienko O and Levi P (2004a) About nature of emergent behavior in micro-systems. In: *Proceedings of the International Conference on Informatics in Control, Automation and Robotics (ICINCO 2004)*, Setubal, Portugal, pp. 33–40.
- Kornienko S, Kornienko O and Levi P (2004b) Generation of desired emergent behavior in swarm of micro-robots. In: Lopez de Mantaras R and Saitta L (eds), *Proceedings of the 16th European Conference on Artificial Intelligence (ECAI 2004)*, Valencia, Spain. Amsterdam: IOS Press, pp. 239–243.
- Kornienko S, Kornienko O and Levi P (2005a) Collective AI: context awareness via communication. In: *Proceedings of the IJCAI 2005*, Edinburgh, UK, pp. 1464–1470.
- Kornienko S, Kornienko O and Levi P (2005b) Minimalistic approach towards communication and perception in microrobotic swarms. In: *Proceedings of the International Conference on Intelligent Robots and Systems (IROS-2005)*, Edmonton, Canada, pp. 2228–2234. DOI: 10.1109/IROS.2005.1545594.
- Leoncini I and Rivault C (2005) Could species segregation be a consequence of aggregation processes? Example of *Periplaneta americana* (L.) and *P. fuliginosa* (serville). *Ethology* 111: 527–540.
- Lioni A, Sauwens C, Theraulaz G and Deneubourg JL (2001) Chain formation in *Oecophylla longinoda*. *Journal of Insect Behavior* 14: 679–696.
- Liu Y, Mu L, Liu B and Kong J (2005) Controlled switchable surface. *Chemistry – A European Journal* 11: 2622–2631. DOI: 10.1002/chem.200400931.
- Martel S, André W, Mohammadi M, Lu Z and Felfoul O (2009) Towards swarms of communication-enabled and intelligent sensotaxis-based bacterial microrobots capable of collective tasks in an aqueous medium. In: *2009 IEEE International Conference on Robotics and Automation*, pp. 2617–2622.
- Martin M, Chopard B and Albuquerque P (2002) Formation of an ant cemetery: swarm intelligence or statistical accident? *Future Generation Computer Systems* 18: 951–959. DOI: 10.1016/S0167-739X(02)00074-2.
- Melhuish C, Holland O and Hoddell S (1999) Convoying: using chorusing to form travelling groups of minimal agents. *Robotics and Autonomous Systems* 28: 207–216.
- Nakagaki T (2001) Smart behavior of true slime mold in a labyrinth. *Research in Microbiology* 152: 767–770.
- Pasteels JM, Deneubourg JL and Goss S (1987) Self-organization mechanisms in ant societies (i): Trail recruitment to newly discovered food sources. *Experientia Supplementum* 54: 155–175.
- Prieto V (2006) *Development of Cooperative Behavioural Patterns for Swarm Robotic Scenarios*. Master Thesis, University of Stuttgart.
- Radspieler G, Thenius R and Schmickl T (2009) Individual based modelling of temperature induced aggregation behavior. In: *MATHMOD 2009 - 6th Vienna International Conference on Mathematical Modelling*, Vienna, Austria, 11–13 February.
- Renshaw E and Henderson R (1981) The correlated random walk. *Journal of Applied Probability* 18: 403–414.
- Schmickl T and Hamann H (2010) BEECLUST: A swarm algorithm derived from honeybees. In: Yang Xiao and Fei Hu (ed.), *Bio-inspired Computing and Communication Networks*. Abingdon: Routledge.
- Schmickl T, Thenius R, Möslinger C, Radspieler G, Kernbach S and Crailsheim K (2008) Get in touch: Cooperative decision making based on robot-to-robot collisions. *Autonomous Agents and Multi-Agent Systems* 18: 133–155.
- Seeley TD (1989) Social foraging in honey bees: how nectar foragers assess their colony's nutritional status. *Behavioral Ecology and Sociobiology* 24: 181–199.
- Seeley TD, Camazine S and Sneyd J (1991) Collective decision-making in honey bees: how colonies choose among nectar sources. *Behavioral Ecology and Sociobiology* 28: 277–290.

- Sumpter DJT and Broomhead DS (2000) Shape and dynamics of thermoregulating honey bee clusters. *Journal of Theoretical Biology* 204: 1–14.
- Theraulaz G, Bonabeau E and Deneubourg JL (1998) Response threshold reinforcement and division of labour in insect societies. *Psychologie Schweizerische Zeitschrift Für Psychologie Und Ihre Anwendungen* 265(1393): 327–332. Available at: <http://www.ulb.ac.be/sciences/use/publications/JLD/136.pdf>.
- Weiss G (ed.) (1999) *Multiagent Systems. A Modern Approach to Distributed Artificial Intelligence*. Cambridge, MA: MIT Press.
- Wilson EO (1980) Caste and division of labor in leaf-cutter ants (Hymenoptera: Formicidae: Atta). *Behavioral Ecology and Sociobiology* 7: 143–156.